REPORT DOCUMENTATION PAGE

Form Approved OMB NO. 0704-0188

1. REPORT DATE (DD-MM-YYYY)	2. REPORT TYPE	3. DATES COVERED (From - To)
24-08-2015	Final Report	1-Aug-2009 - 30-Jul-2015

4. TITLE AND SUBTITLE

Final Report: Research Area 3 - Mathematical Sciences: Multiscale Modeling of the Mechanics of Advanced Energetic Materials Relevant to Detonation Prediction

5a. CONTRACT NUMBER
W911NF-09-1-0330

5b. GRANT NUMBER

5c. PROGRAM ELEMENT NUMBER
611102

6. AUTHORS
Catalin R. Picu, Mark S. Shephard

5d. PROJECT NUMBER

5e. TASK NUMBER

5f. WORK UNIT NUMBER

7. PERFORMING ORGANIZATION NAMES AND ADDRESSES
Rensselaer Polytechnic Institute
110 8th Street

Troy, NY 12180 -3522

8. PERFORMING ORGANIZATION REPORT NUMBER

9. SPONSORING/MONITORING AGENCY NAME(S) AND ADDRESS (ES)

U.S. Army Research Office
P.O. Box 12211
Research Triangle Park, NC 27709-2211

10. SPONSOR/MONITOR'S ACRONYM(S)
ARO

11. SPONSOR/MONITOR'S REPORT NUMBER(S)
56542-MA.14

12. DISTRIBUTION AVAILIBILITY STATEMENT

Approved for Public Release; Distribution Unlimited

13. SUPPLEMENTARY NOTES

The views, opinions and/or findings contained in this report are those of the author(s) and should not contrued as an official Department of the Army position, policy or decision, unless so designated by other documentation.

14. ABSTRACT

This project focused on the development of multiscale models for molecular crystals, with special emphasis on the secondary explosive cyclotrimethylene trinitramine (RDX). Physical understanding related to the molecular scale mechanics of this material was also developed. This data is used as starting point for the definition of physically-based coarse grained models. In turn, these models are to assist the design of new energetic materials with enhanced energy release rates and reduced sensitivity to unintentional detonation. The following results have been obtained: a) we investigated conformational stability of the RDX molecule in the crystal as a function of

15. SUBJECT TERMS

multiscale modeling, molecular simulations, detonation prediction

16. SECURITY CLASSIFICATION OF:			17. LIMITATION OF ABSTRACT	15. NUMBER OF PAGES	19a. NAME OF RESPONSIBLE PERSON
a. REPORT	b. ABSTRACT	c. THIS PAGE			Catalin Picu
UU	UU	UU	UU		19b. TELEPHONE NUMBER 518-276-2195

Report Title

Final Report: Research Area 3 - Mathematical Sciences: Multiscale Modeling of the Mechanics of Advanced Energetic Materials Relevant to Detonation Prediction

ABSTRACT

This project focused on the development of multiscale models for molecular crystals, with special emphasis on the secondary explosive cyclotrimethylene trinitramine (RDX). Physical understanding related to the molecular scale mechanics of this material was also developed. This data is used as starting point for the definition of physically-based coarse grained models. In turn, these models are to assist the design of new energetic materials with enhanced energy release rates and reduced sensitivity to unintentional detonation. The following results have been obtained: a) we investigated conformational stability of the RDX molecule in the crystal as a function of temperature and determined the density of conformers in steady state at temperatures between room and melting, b) we identified the stable dislocations in RDX and, for the first time, established a ranking of slip systems in terms of the Peierls stress (critical stress for dislocation motion), c) we discovered a family of point defects which are rotated and distorted molecules embedded in an otherwise perfect crystal; the stability of such point defects was demonstrated with DFT simulations and a method was proposed to detect them experimentally using Raman spectroscopy, d) we are currently investigating the effect of temperature on the ranking of slip systems, which is a result needed in crystal plasticity models of hot spot formation, e) we developed a family of coarse grained models for the RDX crystal in which the molecules are gradually coarse grained to higher and higher degrees, ranging from full atomistic detail to rigid blobs, and we determined the level of error introduced by coarse graining in various macroscopic measures of crystal thermo-mechanics.

Enter List of papers submitted or published that acknowledge ARO support from the start of the project to the date of this printing. List the papers, including journal references, in the following categories:

(a) Papers published in peer-reviewed journals (N/A for none)

Received		Paper
08/19/2015	9.00	Nithin Mathew, Catalin R. Picu, Peter. W. Chung. Peierls Stress of Dislocations in Molecular Crystal Cyclotrimethylene Trinitramine, The Journal of Physical Chemistry A, (06 2013): 5326. doi: 10.1021/jp401368t
08/19/2015	10.00	N. Mathew, R.C. Picu. Slip asymmetry in the molecular crystal cyclotrimethylenetrinitramine, Chemical Physics Letters, (09 2013): 78. doi: 10.1016/j.cplett.2013.07.057
08/19/2015	11.00	R. C. Picu, A. Pal. Rotational defects in cyclotrimethylene trinitramine (RDX) crystals, The Journal of Chemical Physics, (01 2014): 44512. doi: 10.1063/1.4862997
08/19/2015	12.00	Ting Xie, Seegyoung Seol, Mark S. Shephard. Generic components for petascale adaptive unstructured mesh-based simulations, Engineering with Computers, (10 2014): 79. doi: 10.1007/s00366-012-0288-4
TOTAL:	**4**	

Number of Papers published in peer-reviewed journals:

(b) Papers published in non-peer-reviewed journals (N/A for none)

Received		Paper
08/19/2015	13.00	David E Keyes, , Lois C McInnes, , Carol Woodward,, William Gropp, , Eric Myra, , Michael Pernice, , John Bell,, Jed Brown, , Alain Clo, , Jeffrey Connors, , Emil Constantinescu, , Don Estep,, Kate Evans, , Charbel Farhat, , Ammar Hakim, , Glenn Hammond, , Glen Hansen,, Judith Hill, , Tobin Isaac, , Xiangmin Jiao, , Kirk Jordan, , Dinesh Kaushik,, Efthimios Kaxiras, , Alice Koniges, , Kihwan Lee, , Aaron Lott, , Qiming Lu,, John Magerlein,, Reed Maxwell,, Michael McCourt, , Miriam Mehl,, Roger Pawlowski, , Amanda P Randles, , Daniel Reynolds, , Beatrice Riviere,, Ulrich Rude, , Tim Scheibe, , John Shadid, , Brendan Sheehan, , Mark Shephard,, Andrew Siegel, , Barry Smith, , Xianzhu Tang, , Cian Wilson,, Barbara Wohlmuth. Multiphysics simulations:Challenges and opportunities, High Performance computing applications, (01 2013): 4. doi:
08/30/2013	7.00	Nithin Mathew, Catalin R. Picu, Peter W. Chung. Peierls Stress of Dislocations in Molecular Crystal CyclotrimethyleneTrinitramine, Journal of Physical Chemistry A, (06 2013): 5326. doi:
08/30/2013	8.00	Catalin R. Picu, Nithin Mathew. Slip asymmetry in the molecular crystalcyclotrimethylenetrinitramine, Chemical Physics Letters, (08 2013): 0. doi:
09/07/2011	1.00	Nithin Mathew, Catalin Picu. Molecular conformational stability in cyclotrimethylene trinitramine crystals, Journal of Chemical Physics, (07 2011): 24510. doi:
TOTAL:	**4**	

Number of Papers published in non peer-reviewed journals:

(c) Presentations

1. N. Mathew and R.C. Picu, “Conformational changes in crystalline ?-RDX and associated lattice defects: A molecular dynamics study”, Mini-Symposia on Molecular Modeling of Advanced Materials, USNCCM, Minneapolis, July 2011.

2. N. Mathew and R.C. Picu, “Computational study of conformational changes in a-RDX”, Symposium 9: Computational Nanotechnology, McMat2011, Chicago, May 2011.

3. A. Pal. N. Mathew, R.C. Picu, Dislocations in the molecular crystal RDX: core structures, Peierls stresses and interaction with point defects, US National Congress on Theoretical and Applied Mechanics, Lansing, MI, 2014.

4. W.R. Tobin, D. Fovargue and M.S. Shephard, Parallel Infrastructure for Multiscale Simulations, SIAM Conference on Parallel Processing, Portland, Oregon, February 19, 2014.

5. M.S. Shephard and C.W. Smith, “HPC Simulation Workflows for Engineering Innovation”, XSEDE '14, Jul 13-18 2014, Atlanta, GA, USA ACM 978-1-4503-2893.

6. A. Pal and R.C. Picu, Dislocations and point defects in molecular crystal RDX and their role in initiation, MRS Fall meeting, Symposium VV-Reactive materials, Dec. 2014.

7. W.R. Tobin, D. Fovargue, D. Ibanez, M.S. Shephard, “Adaptive Multiscale Simulation Infrastructure – AMSI”, SIAM Parallel Process Conference, 2014.

8. W.R. Tobin, D. Fovargue and M.S. Shephard, “Load Balancing Multiscale Simulations”, SIAM Conference on Computational Science and Engineering, 2015.

Poster Presentations:

9. N. Mathew and R.C. Picu, “Study of dislocations in ?-RDX using atomistic simulations”, Symposium Y: Advances in Energetic Materials Research, MRS Fall 2011.

10. N. Mathew, A. Pal, R.C. Picu, “Role of conformational and rotational defects in the plastic deformation of molecular crystal RDX,” MRS Fall Meeting, Boston, December 2012.

11. A. Pal, N. Mathew and R.C. Picu, Slip asymmetries and rotational defects in the molecular crystal RDX, APS March Meeting, Denver, CO, March 2014.

Number of Presentations: 11.00

Non Peer-Reviewed Conference Proceeding publications (other than abstracts):

Received	Paper
08/30/2013 5.00	A. Pal, R.C. Picu. Rotational defects and plastic deformation in molecular crystal RDX, American Physical Society March Meeting. 15-MAR-13, . : ,
TOTAL:	**1**

Number of Non Peer-Reviewed Conference Proceeding publications (other than abstracts):

Peer-Reviewed Conference Proceeding publications (other than abstracts):

Received	Paper	
08/30/2013	4.00	Nithin Mathew, Catalin Picu. Relationship between local temperature fluctuations and molecular conformational stability in RDX crystals: A molecular dynamics study, MRS Fall Meeting. 01-DEC-11, . : ,
TOTAL:	**1**	

Number of Peer-Reviewed Conference Proceeding publications (other than abstracts):

(d) Manuscripts

Received	Paper
TOTAL:	

Number of Manuscripts:

Books

Received	Book
TOTAL:	

Received	Book Chapter

TOTAL:

Patents Submitted

Patents Awarded

Awards

R.C Picu, elected Fellow of the American Society of Mechanical Engineers (ASME)

M.S. Shephard, awarded the John Von Neumann Medal by the US Association of Computational Mechanics

M.S. Shephard, 2012 IMR fellow award: The IMR-2012 Fellow Award recognizes an individual with a distinguished record of research accomplishments in the area of Mesh Generation

Graduate Students

NAME	PERCENT_SUPPORTED	Discipline
Nithin Mathew	1.00	
Anitban Pal	1.00	
William Tobin	0.00	
FTE Equivalent:	**2.00**	
Total Number:	**3**	

Names of Post Doctorates

NAME	PERCENT_SUPPORTED
FTE Equivalent:	
Total Number:	

Names of Faculty Supported

NAME	PERCENT_SUPPORTED	National Academy Member
Catalin Picu	0.04	
Mark Shephard	0.02	
FTE Equivalent:	**0.06**	
Total Number:	**2**	

Names of Under Graduate students supported

NAME	PERCENT_SUPPORTED	Discipline
Daniel R. Kimball	0.10	Computer Science
Sean P. Kilner	0.10	Computer Science
FTE Equivalent:	**0.20**	
Total Number:	**2**	

Student Metrics

This section only applies to graduating undergraduates supported by this agreement in this reporting period

The number of undergraduates funded by this agreement who graduated during this period:	2.00
The number of undergraduates funded by this agreement who graduated during this period with a degree in science, mathematics, engineering, or technology fields:	2.00
The number of undergraduates funded by your agreement who graduated during this period and will continue to pursue a graduate or Ph.D. degree in science, mathematics, engineering, or technology fields:	0.00
Number of graduating undergraduates who achieved a 3.5 GPA to 4.0 (4.0 max scale):	2.00
Number of graduating undergraduates funded by a DoD funded Center of Excellence grant for Education, Research and Engineering:	0.00
The number of undergraduates funded by your agreement who graduated during this period and intend to work for the Department of Defense	0.00
The number of undergraduates funded by your agreement who graduated during this period and will receive scholarships or fellowships for further studies in science, mathematics, engineering or technology fields:	0.00

Names of Personnel receiving masters degrees

NAME
Total Number:

Names of personnel receiving PHDs

NAME	
Nithin Mathew	
Anirban Pal	
Total Number:	**2**

Names of other research staff

NAME	PERCENT_SUPPORTED
FTE Equivalent:	
Total Number:	

Sub Contractors (DD882)

Inventions (DD882)

Scientific Progress

The main results of this work are:

a) identified conformational stability of RDX molecules in the crystal and its dependence on temperature,
b) identified the stable dislocations in RDX,
c) established a ranking of slip systems in terms of the Peierls stress at zero Kelvin. We are currently investigating the effect of temperature on this ranking,
d) discovered a family of rotational defects (point defects) in RDX,
e) developed a family of coarse grained models of the RDX crystal.

We outline briefly the central results and their significance. The discussion here refers to the attached file which contains actual data and schematic representations.

a) Conformational stability of RDX molecules

The RDX molecule exists in the form of 4 conformers denoted by Caae, Caee, Caaa and Ceee. The molecule is composed from a triazine ring and three nitro side groups (Slide 1). The side groups take positions that make angles ranging from approximately 35o to 135o with respect to the normal of the ring. An angle of 90o corresponds to an equatorial position (denoted by 'e'), while angles close to the extremes of the indicated range correspond to axial positions (denoted by 'a'). A conformer of Caae type has one nitro group in the equatorial position, and two nitro groups in the axial position (Slide 2). The transition of a nitro group between a and e states is limited by potential barriers (Slide 2).
Relevance of conformer transitions in the crystal. We determined that the molecules do not change state in the crystal at room temperature and in absence of loads. Transitions take place when either tension (uniaxial or biaxial) or compression are applied. Under such conditions, molecules change state by switching from Caae (the ground state) to Caee and back. In doing so, they absorb phonons with energy at least equal to the height of the barrier between the two states. This energy is released in the form of molecular vibrations when the structure "falls from the height of the barrier" into the new potential well (corresponding to the conformer). The same process happens when the molecule transforms back from Caee to the ground state. We have seen (Slide 5) that this leads to localized heating of the respective molecule by ~10K. Hence, the molecule temperature increases immediately after the transition and then decreases gradually (ps time scale) by thermalization.
Effect of strain/stress. It has been observed that conformers are not stable in the unloaded alpha-RDX crystal. However, we determined that a fraction of the Caae molecules transform to Caee if the crystal is stretched in the [001] crystallographic direction. Interestingly, stretching in other crystal directions, as well as applying a hydrostatic strain does not promote the transformation (Slide 3).
Correlated dynamics of conformal transitions. Since a conformer induces a long-range strain field, neighboring conformers interact. We evaluated the range of interaction (which is quite large: conformers interact even when separated by 17A) and determined that a) conformers cluster in space (i.e. transition from the ground state to Caee is favorable in the vicinity of a molecule which has already transformed), b) conformational changes between Caae and Caee are correlated in time (Slide 4). Both spatial and temporal correlations are attributed to the field-mediated interaction of these "point defects." Observation a) is relevant for the concentration of the kinetic (thermal) energy on the molecular scale. As discussed above, when an isolated molecule transforms between conformer states, its effective temperature (kinetic energy) increases by approximately 10K. If multiple molecules in a region of the crystal perform similar transitions, the temperature of a larger region of the crystal increases. This fluctuation lasts longer than the temperature fluctuation resulting when a single molecule transforms since thermalization takes longer when a larger volume of material is involved.

b) Stability of dislocations in RDX

Initiation and detonation happen as a consequence of plastic deformation and/or overheating. In this work we investigated the mechanisms by which plastic deformation takes place in RDX.
RDX, with its complex crystal and molecular structure, is generally considered elastically soft, but plastically hard. This is a consequence of the relatively soft inter-molecular bonding and is a common feature in molecular crystals. It has been shown experimentally that the easiness of slip in certain directions correlates with initiation. In this work we aimed to identify the active slip systems and to rank them in terms of dislocation mobility such to help make this statement quantitative.
It results that in many slip systems in which dislocations could –in principle- form, plastic deformation is actually sluggish since either only dislocations with large Burgers vectors exist, or the stable dislocations have high Peierls stresses. To clarify on which crystallographic planes and directions dislocations can form, we focused on investigating the core-structures of edge and screw dislocations in various experimentally reported slip systems for RDX. Experimental studies suggest the occurrence of slip on the {021}, {011} and (010) planes. In addition to these, the slip plane (001) was also considered. The crystal structure of RDX permits slip in two parallel planes for each type. In our investigations, the plane with lower attachment energy was selected. Calculations of the dislocation energies were done using an atomistic model using the Smith-Bharadwaj potential. Slide 6 shows a (100) projection of the RDX crystal in its ground state and the slip systems which produce slip in the [100] direction. Note that several glide planes may produce this type of slip and the associated dislocations can be edge or screw. Slides 7, 8 and 9 show core structures for various glide planes and dislocation types. The cores are generally narrow and splitting of dislocations in partials is rarely observed. The narrowest core is seen for the (011) [100] system with a width of

approximately 3*l100., where l stands for the unit cell in the respective direction. The (010) and (021) edge dislocations in the [100] direction have fairly wide cores with a width of 6* l100. An interesting feature can be observed for the (001) [010] edge dislocation where the stable core has a width of about 5*l010 and develops out of plane screw component.

c) Ranking of slip systems

The central result related to dislocation mechanics, which is the physical basis of plasticity, is the ranking of slip systems. The potentially active slip systems have been identified using atomistic models (section (b)), but some of these systems host essentially sessile dislocations and are effectively inactive. To clarify which slip systems are actually active one has to evaluate the Peierls stress, i.e. the stress required to move dislocations in the perfect crystal. These stress values represent the lower limit of the stress required for plastic deformation in the various crystallographic planes and directions. They can be used to determine which systems are active and whether a sufficient number of systems exist to render plastic deformation feasible macroscopically. The importance of this result from a modeling/computation standpoint is that in coarse grained dislocation dynamics (DDD) simulations, one needs to input the Peierls stress which enters the equation of motion of dislocations. Hence, the study performed here represents a sequential scale linking step in this multiscale analysis of plasticity in RDX.
Slide 10 shows the Peierls stress values calculated using a large scale atomistic model. The 4 types of symbols correspond to 4 slip planes which are considered to be active in RDX. In each plane one may have edge and screw dislocations and these may have full or half Burger vector. The notation “e1/2[100]”, for example, stands for the edge dislocation with Burgers vector ½ of the full Burgers vector in the [100] direction of the crystal. The horizontal axis shows the theoretical strength of the respective systems computed based on the shear modulus in the respective crystal direction. It is seen that the system with lowest Peierls barrier is the ½[100] system, in which both the screw and edge dislocations have critical stresses about an order of magnitude smaller than the theoretical strength.
Slide 11 shows some of the implications of the ranking of slip systems in Slide 10. The figure on the left shows the resolved stress in all systems activated by shocks applied in specific crystal directions and of specific magnitudes. Shock of three magnitudes (from 1.24 to 7 GPa) have been applied in experiments perpendicular to the (111) plane. The symbols indicate the resolved stress versus the Peierls stress for all systems activated by this shock. The line has slope 1, such that if a point is above the line, the respective system is active. It is seen that for a shock of magnitude 1.24 GPa, all points are below the line and hence there is no plasticity. For a shock of 7 GPa all points are above the line and one has plastic deformation in all systems. In experiments it is seen that detonation happens when the shock magnitude is larger than 2 GPa. Here we see that when this parameter increases from 1.24 to 2.14 GPa, the points move above the line and more systems are activated. Hence, the data are in good agreement with the experimental, macroscopic observations and suggest that plasticity is intimately related to detonation. The figure on the right shows a similar comparison, with a set of indentation experiments published in the literature. The three types of symbols correspond to indentations in different directions. The data points correspond to slip systems that may be activated by the respective indentation. If the point is above the line, the respective system is indeed activated, i.e. the applied stress is larger than the Peierls stress. These results are compared with direct observations of activation of plastic deformation in specific clip systems in these experiments.
We are in the process of evaluating the temperature dependence of this ranking. The work will be completed after the end date of the current project and is part of the PhD thesis of one of the students supported from the project (Anirban Pal). It may turn out that as the temperature increases, some slip systems which are not active at temperatures close to zero Kelvin, become more active than others that proved to have lower Peierls stress at 0K. Hence, due to the fact that the energetic barriers involved have different height, the ranking at room temperature may be quite different from that reported here (Slide 10). This information is central for the calibration of crystal plasticity models.

Slip asymmetry

Slip asymmetry is a common occurrence in some monatomic crystals where it is due to complex core structures or specific packing of slip planes. We identified a new mechanism, based on molecular steric hindrance, which leads to asymmetric dislocation motion in RDX. Dislocations move at different critical stresses when shear is applied in the positive and negative directions of the Burgers vector in the slip system that contributes most to plastic deformation. This is a new physical observation which has significant implications for coarse grained DDD modeling of plastic deformation.
Slide 12 shows a close-up view of the crystal in the [001] projection. The glide planes of interest are horizontal in this view. Molecules are shown by lines connecting the atomic positions, while spheres represent the positions of the center of mass of the molecules. It is clear from the COM representation that there are two distinct slip planes of the (010) type, which differ in inter-molecular bonding across the glide plane. These planes are denoted as P1 and P2. The interface between the red and blue layers is the P1 slip plane and the interface between the orange and blue layers is the P2 plane. Across the P1 plane the nitro group of the molecules below is oriented in the first trigonometric quadrant. However, it is observed that the P1 plane below the P2 plane indicated in the figure is not identical to the P1 plane above P2. In this case, the nitro groups are pointing in the second quadrant. Therefore, one has two types of P1 planes which are denoted as P1 and P1’. A similar situation exists for the other plane and two variants, P2 and P2’, are defined.
The simple inspection of the crystal geometry is sufficient to suggest the existence of slip asymmetry. To quantify the effect, we compute the Peierls stress for dislocations moving in the two directions for all these (010) planes. The [100] direction pointing to the right in Fig. (b) on slide 12, is denoted as S+ and the opposite direction is denoted as S-. Motion in S+ requires moving the

upper molecular planes to the right relative to the lower planes, in this figure. The resolved shear stress required for motion in the S+ and S- directions in the P1 plane is 0.157 GPa and 0.332 GPa, respectively, with an uncertainty of 0.017 GPa. This indicates that dislocation motion in these planes is asymmetric if the applied stress level is below the largest values of the Peierls stress. The similar analysis performed for the two directions of dislocation motion in the P2 plane leads to a smaller Peierls stress and a smaller asymmetry. Specifically, we obtain 0.201GPa and 0.263GPa with an uncertainty of 0.012 GPa, for the S+ and S- directions, respectively.

d) Rotational defects in RDX

We identified a new type of point defect in molecular crystals: rotational defects. In this case, the molecules are positioned at the proper sites of the crystal, but are rotated relative to their neighbors. A rotational defect completely breaks the point symmetry at the respective site, which is different from other types of molecular rearrangement reported in other molecular crystals. Such rotated molecules are stable only if the steric hindrance of the surrounding molecules helps preserve them in the rotated positions.

To identify whether this is possible, we considered a perfect RDX crystal in which a molecule was rotated to various positions, in different directions relative to the neighboring molecules. The system was then relaxed to determine whether the rotated molecule is stable. This is shown schematically in Slide 13. The figure represents a map of possible molecular rotations. The rotations are characterized by the angles made by the normal to the ring, as shown in the small figure next to the map on slide 13. A state of the molecule is shown by a point on this map. Upon relaxation, the molecule converts to another structure and orientation – this process is represented with an arrow that connects the initial and final states of the relaxation process in this phase space. Note that several attractors appear, i.e. many rotated states convert to a small number (5) of states.

These rotated states are stable at low temperatures. Upon annealing at room temperature, all these rotational defects disappear and the perfect crystal is recovered (state denoted by E). We computed the energy barriers for the formation of these defects and for their conversion back to the perfect crystal state. The barriers for defect formation are on the order of 1.5 eV, while those for their annealing (return to the perfect crystal state) are about 0.3 eV. The formation energy of the various defects is in the vicinity of 1 eV. This indicates that: a) the formation energy is smaller than the formation energy of vacancies (i.e. the density of rotational defects should be larger than that of vacancies), b) thermal fluctuations are insufficient to produce rotational defects at all temperatures at which the solid phase of RDX exists, c) the 0.3 eV barrier determines a characteristic survival time which is temperature dependent (i.e. if the defect is formed but the conditions leading to its formation are eliminated at t=0, the time interval after which the molecule rotates back to the perfect crystal orientation is determined by this “return barrier”).

Slide 14 shows the 4 rotated conformations which are stable in addition to the perfect crystal state. These correspond to the 5 attractors shown in the map of slide 2 (labeled A to E), of which state E is the perfect crystal (not shown on slide 14).

Thermal fluctuations are not expected to produce a sizable number of such defects. However, we have identified them in dislocation cores. Two dislocation core images showing rotated molecules (colored) are shown on slide 15. Therefore, we envision that rotational defects are formed in cores and, as dislocations move away, are left behind in the perfect crystal. Thermal fluctuations anneal them back in a characteristic time defined by the 0.3 eV return barrier; this time is on the order of microseconds. This is long enough for these defects to interact with phonons and other dislocations moving in the same glide plane. The importance of rotational defects to plasticity and phonon scattering follows from this observation.

Relevance for initiation. We have used first principle calculations (plane wave Density Functional Theory with projector augmented-wave (PAW) pseudopotentials and the Perdew-Burke-Ernzerhof (PBE) exchange-correlation functional implemented within the generalized gradient approximation (GGA) in VASP) to verify the atomistic results presented before and to determine the electron density.

It has been established that thermal decomposition in solid a-RDX begins with N-N bond scission. Therefore we examined how electronic charge is distributed in the N-NO2 region of the defect molecules. If charge deficiency over the N-N bond is considered to be an indicator of sensitivity, one needs to only focus on the most charge deficient N-N bond in the molecule. In addition, since only one NO2 group is lost per molecule during decomposition, the N-N bond with the least covalent character can be expected to constitute the initial fission center. Slide 16 shows the charge distribution along 2-D slices of the most deficient N-NO2 groups for the defect and perfect molecules. For the perfect crystal case (labelled E), the charge density along an axial N-NO2 group is shown, and one can see that the electron density at the mid-point of the N-N bond is non-zero. However, all four defects (A-D) show some charge deficiency at the mid-points of the N-NO2 bonds, suggesting that these defect molecules may be more sensitive to decomposition. More quantitatively, in the perfect crystal (E) the minimum density along the N-N bond is 0.327 e Bohr-3. For the defect molecules A-D, the N-N electron density minimums are 0.309, 0.288, 0.318, and 0.301 e Bohr-3 respectively.

How to identify experimentally rotational defects? To assist the experimental identification of rotational defects, we computed the eigenfrequencies of the crystal containing the 4 types of rotational defects described on slide 14 in a region of high frequencies where the spectrum of the perfect crystal has sparse bands. The figure on slide 17 shows the perfect crystal frequencies with black bands and arrows. The colored bands correspond to the various defects. As seen, band splitting occurs in presence of rotational defects and this can be used to identify them using Raman spectroscopy.

e) Coarse grained models

Two models of the RDX (and HMX) molecule exist at present in the open literature: the fully explicit atomistic model in which all

atoms are represented and the fully rigid molecule developed by B. Rice's group at ARL. The reference model is, of course, the explicit, atomistic model. It has been shown that the rigid model is unable to capture some important features of the mechanics of this crystal. Specifically, the predicted stacking fault energies are incorrect and the dislocation cores are no stabilized by this model. On the other hand, any coarse grained model which uses larger coarse graining levels is not going to represent dislocations explicitly for the simple reason that such models do not represent explicitly all molecules of the crystal. Hence, the coarse graining level that can capture the atomistic mechanics right and hence is acceptable should be lower than the fully rigid molecule.

In this work we developed a family of models that interpolate between the fully flexible (explicit atomistic model) and the rigid molecule. Their ability to capture specific material parameters important in the mechanics of the crystal has been tested. Slide 18 shows the 5 models of this family. Model I corresponds to the fully flexible molecule, while model V corresponds to the fully rigid molecule. In model II the nitro groups are rigid and the bonds connecting the nitro group to the ring are also inextensible. The rest of the molecule is flexible. Model III is similar to model II, except that the bonds (C-C and C-N) of the ring are also made inextensible. In Model IV, the whole ring is made rigid while the rigid nitro groups are free to flop about the ring. In Model V, the entire molecule is a rigid object.

Slide 19 shows the elastic constants of the crystal predicted with the 5 models. Models II and III give results close to the reference (model I). Once the ring is made rigid (model IV), all elastic constant depart from the reference by about 10%. The error is larger when the rigid model is used.

The lattice parameters are less sensitive to coarse graining. Models III, IV and V lead to errors (relative to the reference, model I) of about 2%. The pressure dependence of the elastic constants (relevant for shock) is the same for all models. This result is shown in slide 20 for one of the lattice parameters.

The coefficient of thermal expansion (CTE) was quite sensitive to coarse graining, as it depends on phonon mode populations and coarse-graining directly affects the normal mode distribution. Models II and III gave similar values (relative to the reference) for the CTE in [100] and [010] directions, but increased by about 20% for the [001] direction. The error for Models IV and V were more pronounced, going as low as 50% of the reference CTE value for the [001] direction. Slide 21 shows the normalized CTE for the 5 models.

These models indicate qualitatively the degrees of freedom that need to be active for accurate thermal and elastic behavior. Each successive model offers the promise of lower computational cost
(in terms of degrees of freedom), while also reducing the physics that can be captured accurately. In this context, Model III seems to offer a good balance of features. The nitro groups can be coarsened out into rigid objects, but the ring has to stay flexible (as shown by poor performance of models IV and V). This study provides a lower bound on the amount of coarse-graining that can be done without sacrificing the accuracy with which the physics is represented.

Summary statement

To summarize the main advances made in this project and their importance in multiscale modeling:

1) The identification of active slip planes using atomistic models is of importance for crystal plasticity models of plastic deformation. In current models, plastic deformation is considered to take place in all systems of the respective crystal type. We have seen that on some systems dislocations are simply not stable and hence these systems should not be considered at all.

2) Ranking of the slip systems is also important for modeling plastic deformation on larger scales. Current mesoscale models have no input regarding the 'friction stress' (one of the components of the equation of evolution of plastic strain in given system) in the various slip systems. This work provides quantitative information in this sense.

3) Rotational defects were described for the first time. We quantified their potential importance in initiation.

4) A family of coarse grained models has been developed for RDX and it was shown that coarse graining the entire molecules in blobs does not lead to accurate results. As long as discrete coarse grained models are to be used, model III described above is the highest level of coarse graining acceptable.

Technology Transfer

This work was performed in collaboration with the groups of Dr. Betsy Rice and Peter W. Chung from the Army Research Labs. Dr. Rice is specialized in quantum mechanical and atomistic modeling of energetic materials. Our contribution was to add physical understanding and to extend the range of scales accessible to their models, which include atomistic (nano) and coarse grained/mesoscale (micro) models. We interacted closely with Dr. Peter Chung (from the Computational & Information Sciences Directorate of ARL until Spring 2014) who has contributed significantly to the work on the Peierls stress of dislocations in RDX which has been published in 2013. This work initiated as a result of our visit to ARL in April 2011 and was discussed in subsequent meetings at RPI. Dr. Chung has served in the PhD committee of Nithin Mathew. Nithin graduated in January 2013.

In April 2014 we visited the group of Dr. Betsy Rice at ARL and gave a talk on the results of the work reported here. This led to the invitation to submit a proposal for the initiation of a Cooperative Agreement with ARL. The proposal has been approved. The Cooperative Agreement provides a framework for sharing information (model development and physical results) between ARL and RPI and provides access to the RPI group to the ARL supercomputing.

We have also interacted with Dr. Plimpton from Sandia National Labs. Dr. Plimption is the primary developer of the LAMMPS molecular dynamics software. We worked together on specific extensions of LAMMPS.

Both the PI and the Co-PI contributed in the past to another project (STTR) involving ARL and Simmetrix Inc., project focused on the development of multiscale modeling technologies for nanomaterials. The tools developed part of this project are currently implemented at ARL and have been used in the current work both at ARL and RPI.

The two PIs worked jointly on a project sponsored by IBM focused on the development and use of multiscale technologies for the purpose of identifying conditions for defect nucleation in microelectronic devices. The broader goal of this set of technologies is to bridge the gap between fabrication and device performance and reliability (“front end” and “back end”).

The PIs were also involved in the past with two NSF-funded projects on multiscale modeling of polymer-based nanocomposites, each funded over a duration of 3 years at levels above $500,000.

A three-year NSF project ($325,000 total funding) on the continued development of the RPI’s AMSI multiscale computing framework ends in July 2015.

Energetic materials are molecular crystals

Chemical structure of the RDX molecule

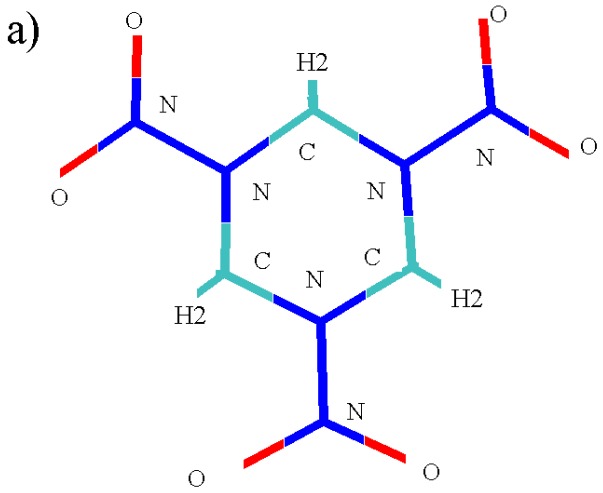

Single molecule
Red = Oxygen
Blue = Nitrogen
Cyan = Carbon
White = Hydrogen

Structure of α-RDX crystal

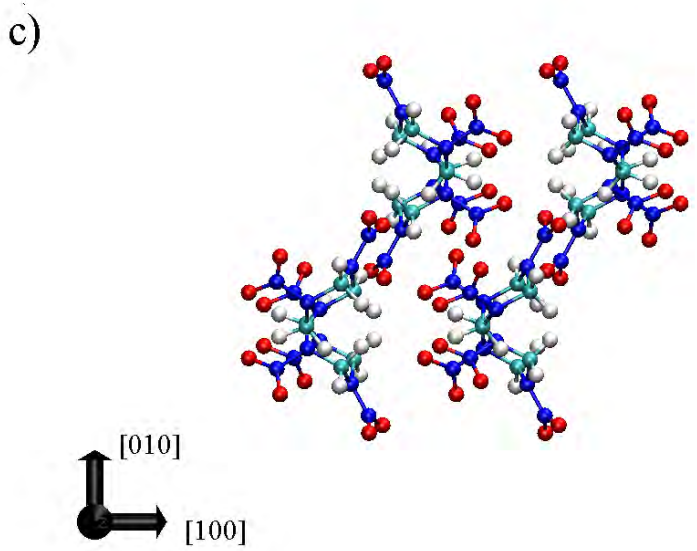

(orthorombic – [100] projection)

(a) Conformational defects in RDX -what are conformers?-

- Estimation of energy barriers using the Nudged Elastic Band method.
- Various conformations stabilized by the Grant-Smith potential are considered.

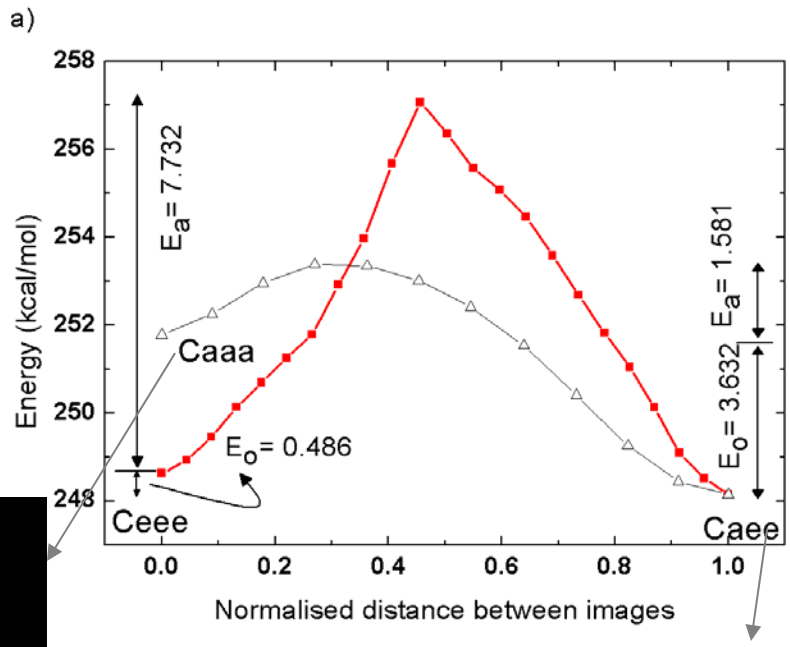

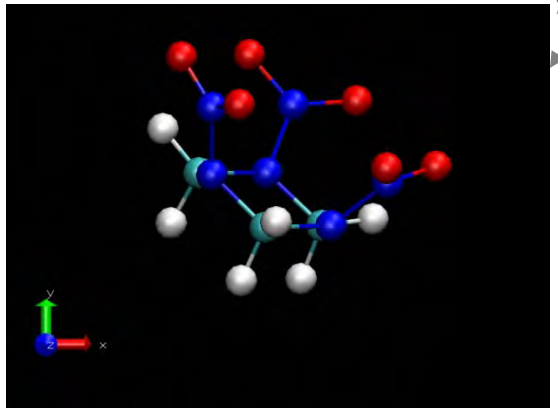

Caaa conformer

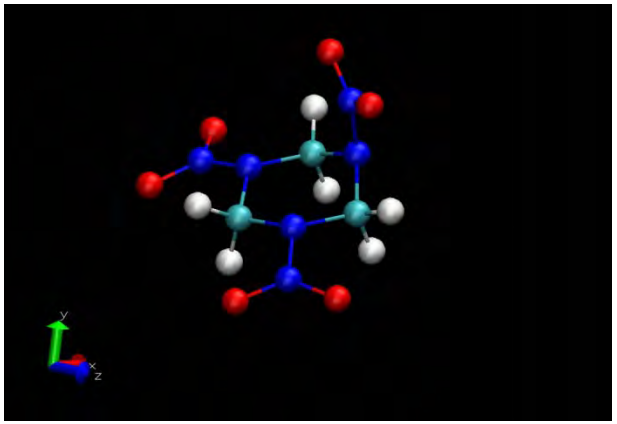

Caee conformer

(a) Conformational defects in RDX -in α-RDX a fraction of molecules are conformers -

• α-RDX is composed from molecules in the Caae state.

• Under uniaxial tensile (and compressive) loading in the [001] direction (as indicated in the figure), a fraction of Caae molecules convert to Caee.

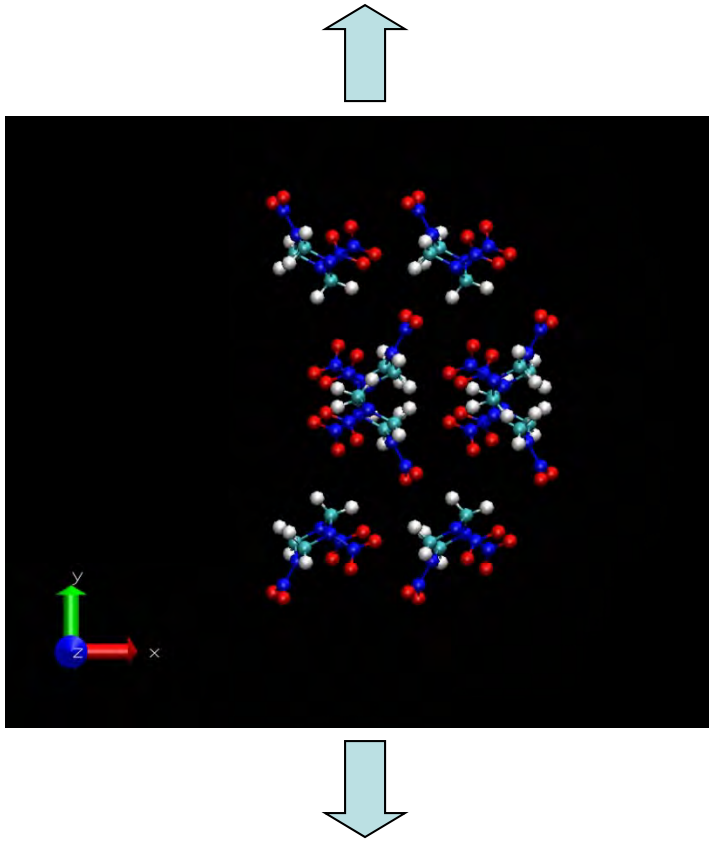

Concentration of Caee after imposing a step strain of 0.7% in [001]. The inset shows the dependence of the stable Caee concentration (fraction) with strain.

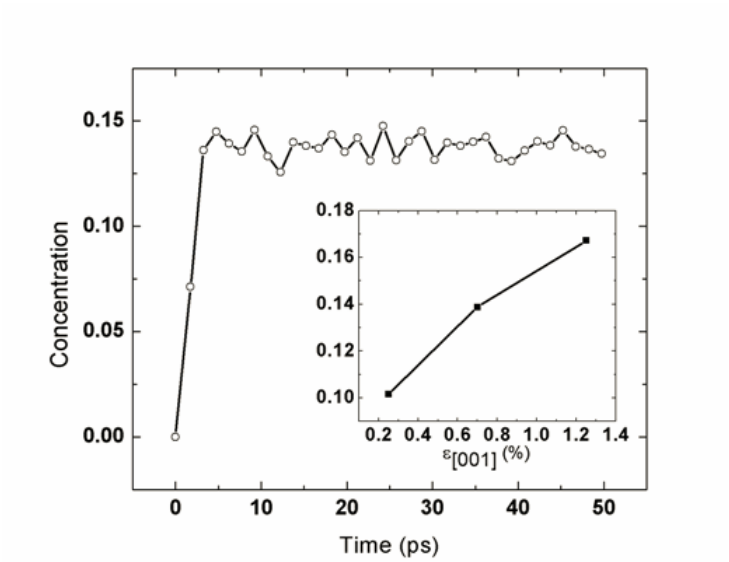

(a) Conformational defects in RDX -conformers tend to cluster in space and transitions tend to cluster in time -

Transformation from Caae to Caee and back is a stochastic process. However, the events are spatially and temporally correlated. This is expected to be important for the mechanism of thermal energy concentration and hot spot formation.

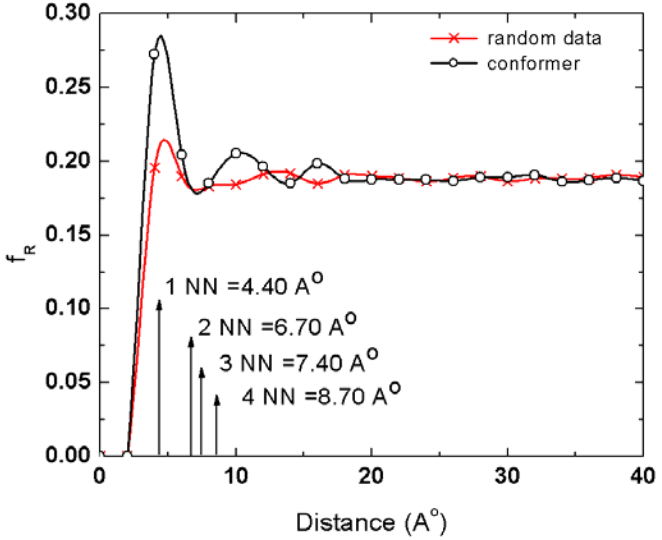

Pair distribution function of Caee molecules indicating clustering of transformation events in the crystal.

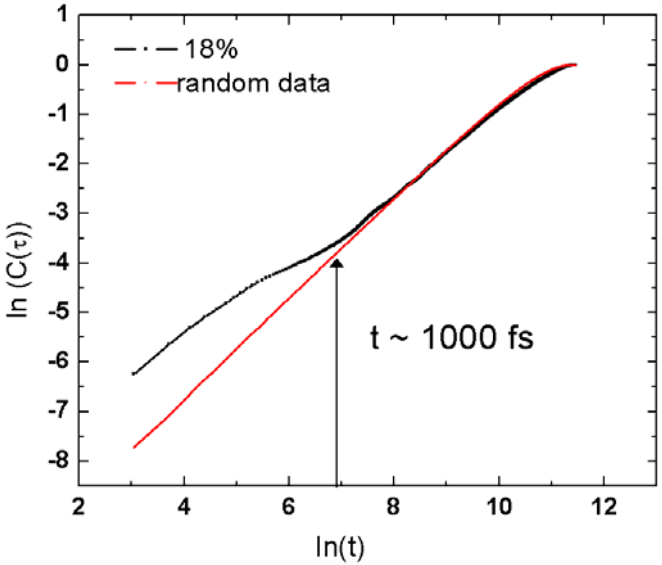

Correlation integral analysis of time series of Caae to Caee transitions indicating temporal correlations. The range of these temporal correlations is approximately 1 ps.

(a) Conformational defects in RDX -a transition leads to local temperature fluctuations-

"Temperature" of intramolecular vibration modes following conformation transitions of a single molecule in the RDX crystal

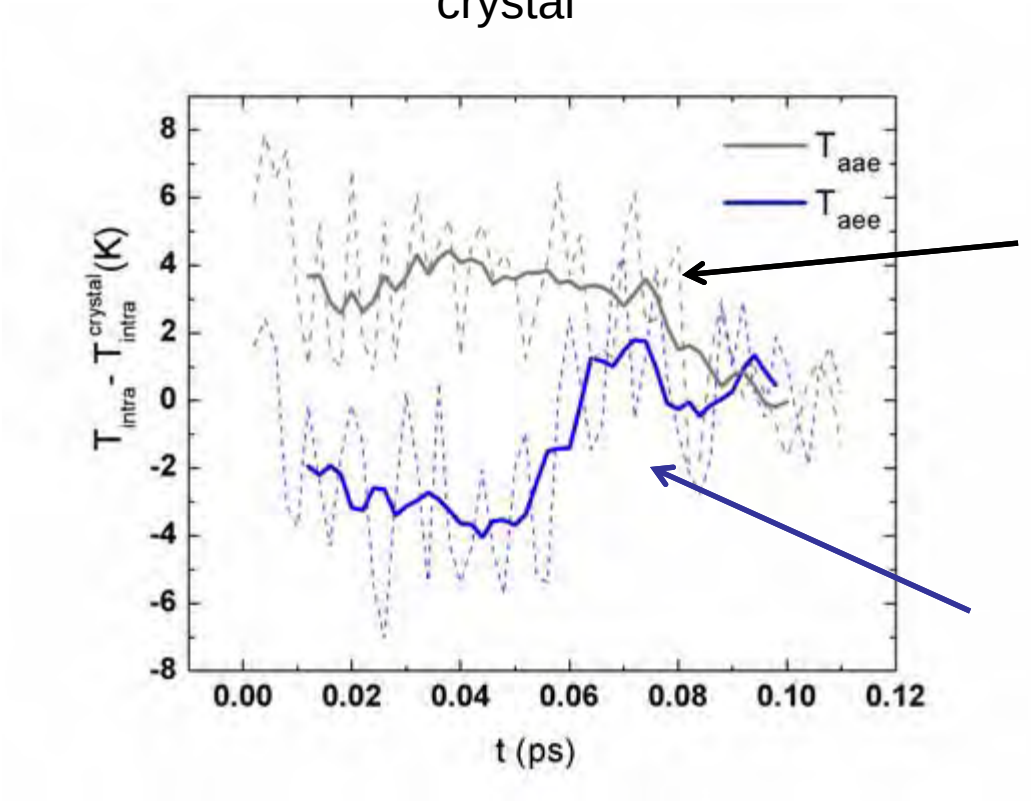

Molecule in Caae after transition from Caee at t = 0

Molecule in Caee after transition from Caae at t = 0

(b) Stability of dislocations in RDX -family of crystallographic planes on which slip occurs-

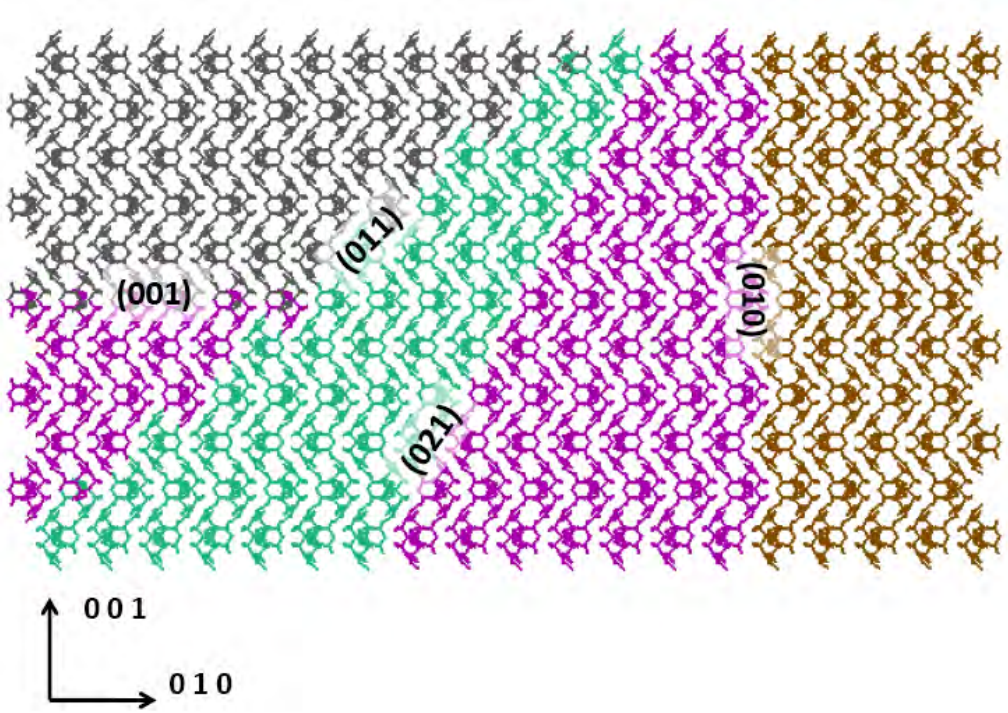

(100) projection of RDX crystal structure indicating the slip planes in which glide can happen in the [100] direction (perpendicular to the figure).

• Slip on (001), {021}, {011} planes has been reported in experimental studies. Note that direct observations of dislocations in RDX is not possible. Computer simulations can clarify the preferred glide systems, the mobility in various glide systems, the Peierls barriers to motion.

(b) Stability of dislocations in RDX -specific stable types of dislocations-

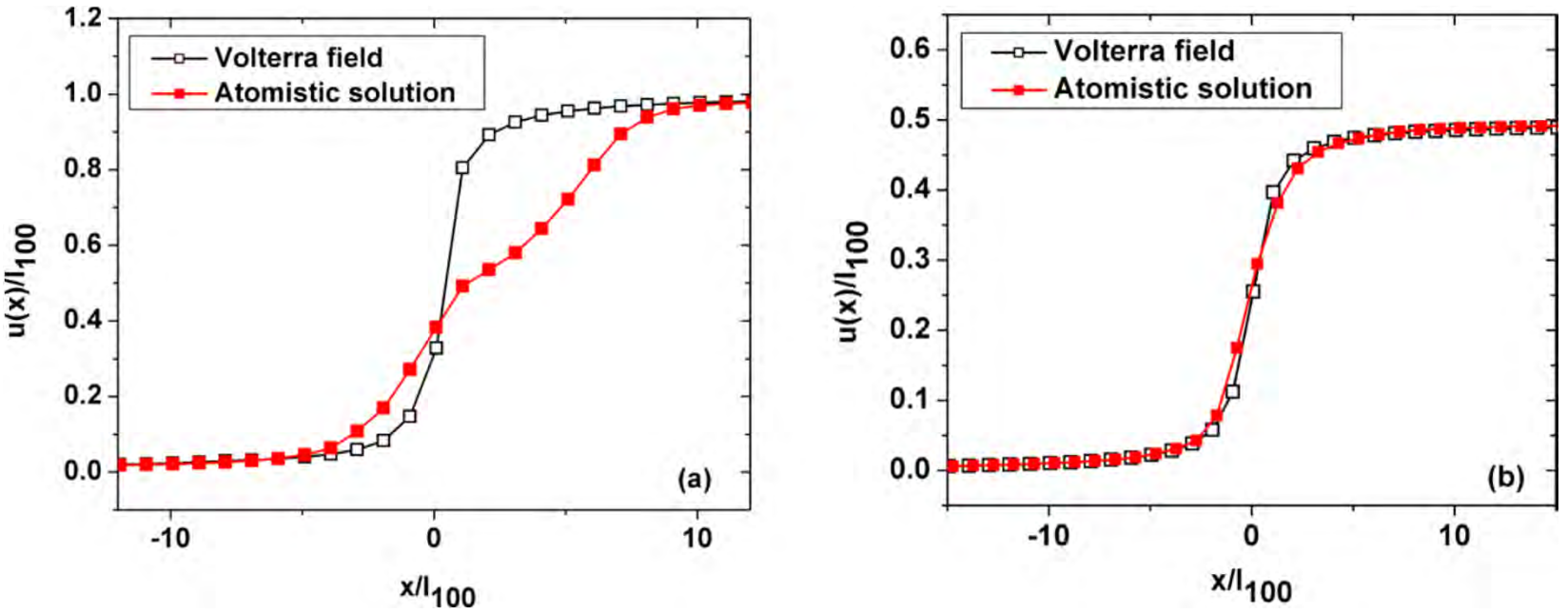

Structure of the (010)[100] edge dislocation. (a) The dislocation with b = [100] splits into two partials of b = 1/2[100]. (b) Structure of the b = 1/2[100] partial.

The (010)[100] screw configuration was found to be unstable.

(b) Stability of dislocations in RDX -specific stable types of dislocations-

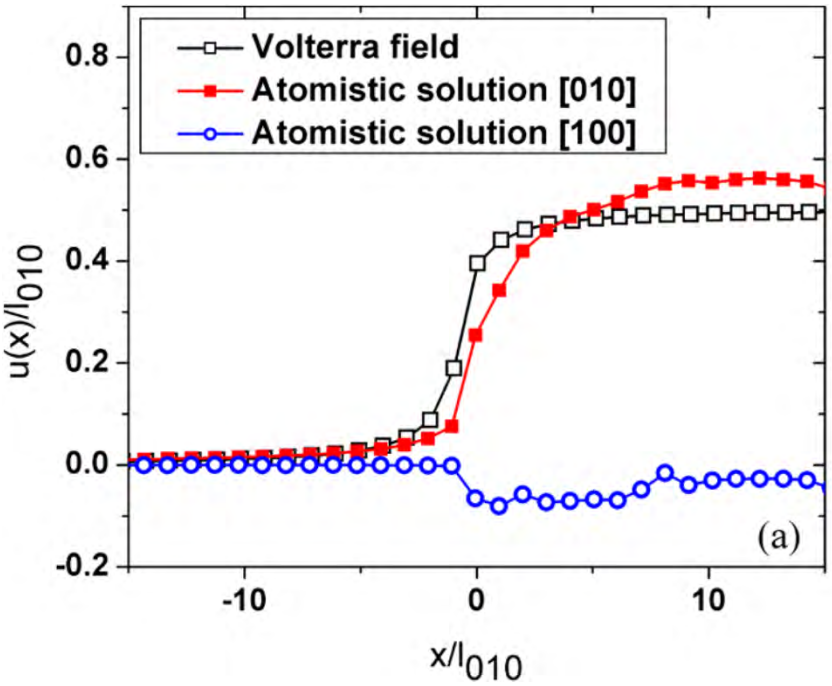

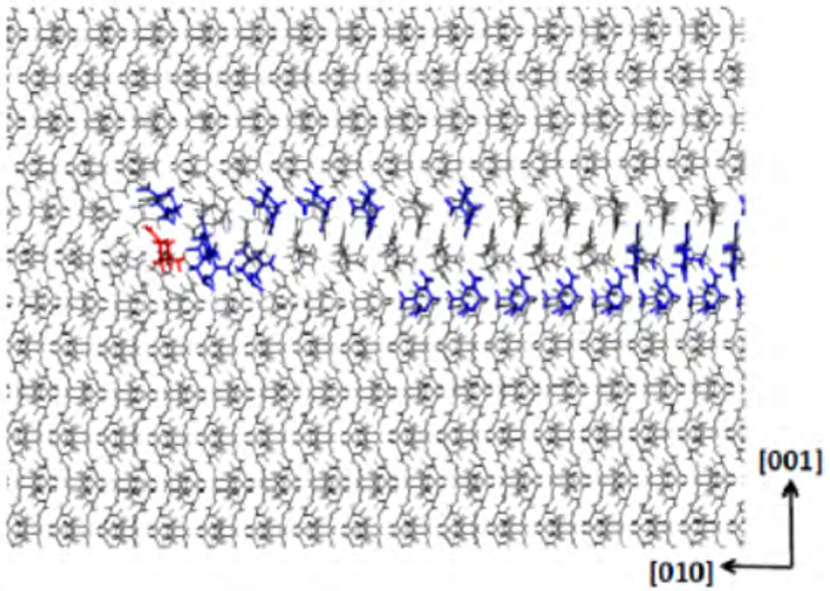

(b)

Core structure of the (001)[010] edge dislocation with b = 1/2[010].
(a) Relative displacement of COM across the glide plane. Note the occurrence of the screw component (blue curve)
(b) Molecular conformational state of the core in (a). Caaa molecules are colored in red, Caee are in blue, and Caae are in gray.

(b) Stability of dislocations in RDX -specific stable types of dislocations-

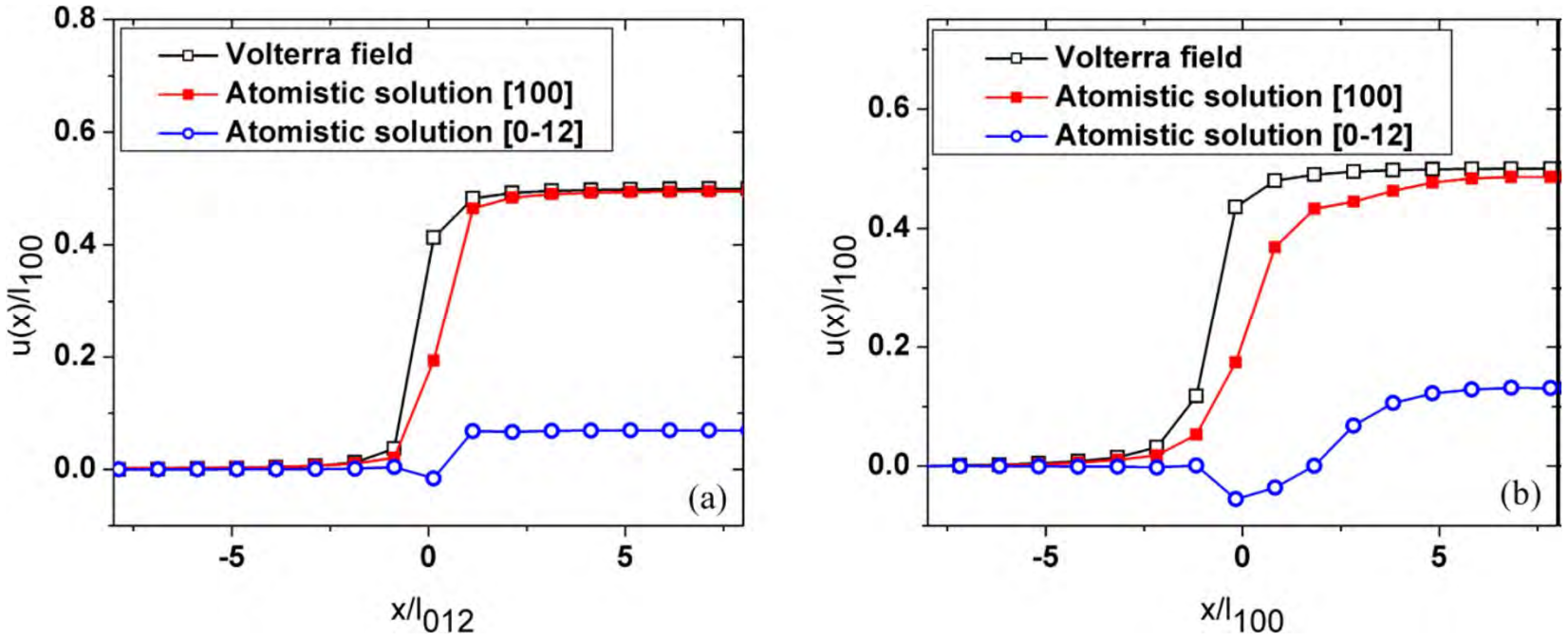

Core structure of b = 1/2 [100] dislocations residing on the (021) plane.
(a) Screw dislocation (b) Edge dislocation

(c) Ranking of slip systems in RDX -Peierls stress values-

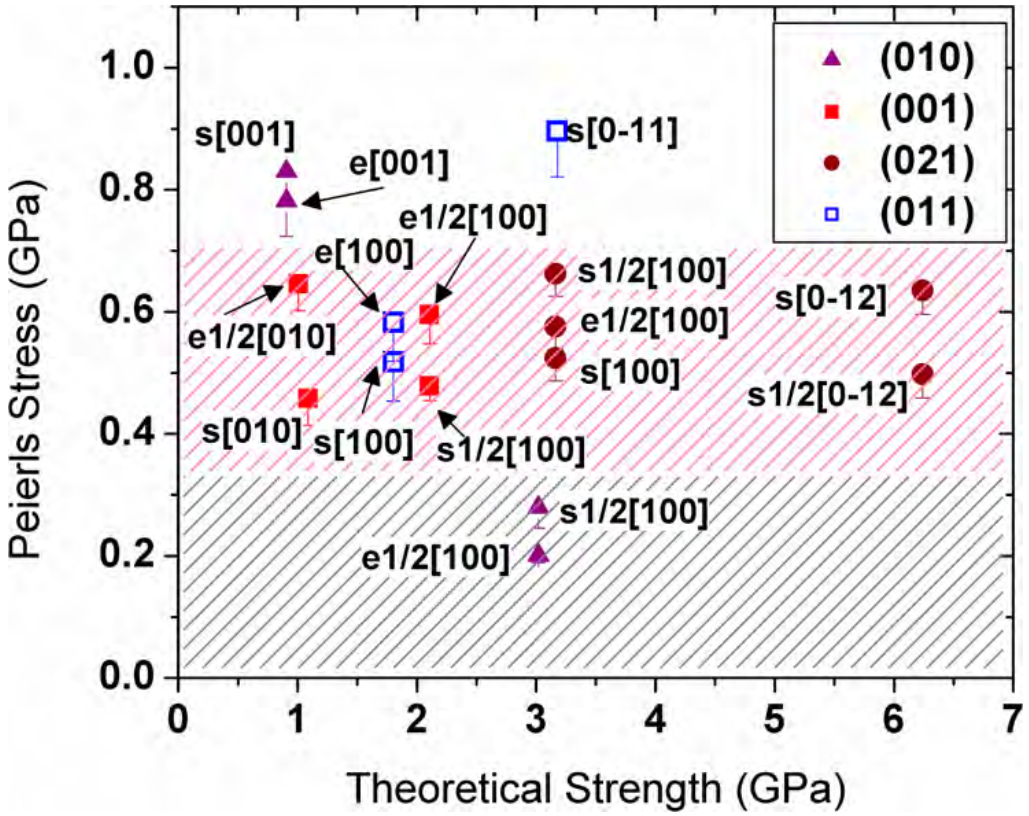

Labels “e” and “s” stand for edge and screw dislocations. The bars represent the range in which the Peierls stress is observed. The limits defining the two shaded areas are selected arbitrarily to correspond to Gv/20 and Gv/10, where Gv is the Voigt shear modulus.

(c) Ranking of slip systems in RDX -Implications of the ranking-

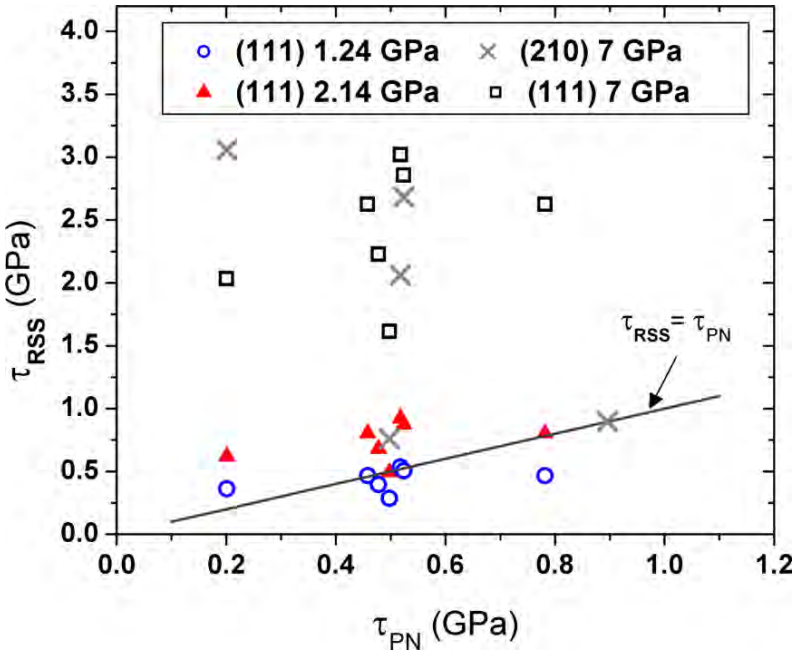

Activation of slip systems for (111) and (210) shocks

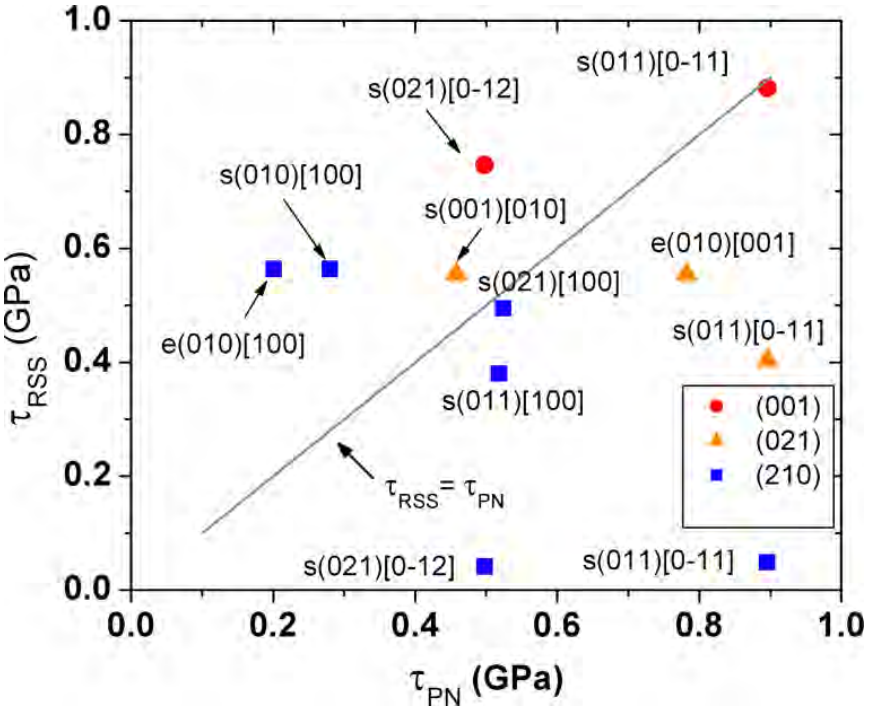

Activation of slip systems in indentation experiments perpendicular to the (001), (021), and (210) crystal planes

(c) Ranking of slip systems in RDX
-Slip asymmetry-

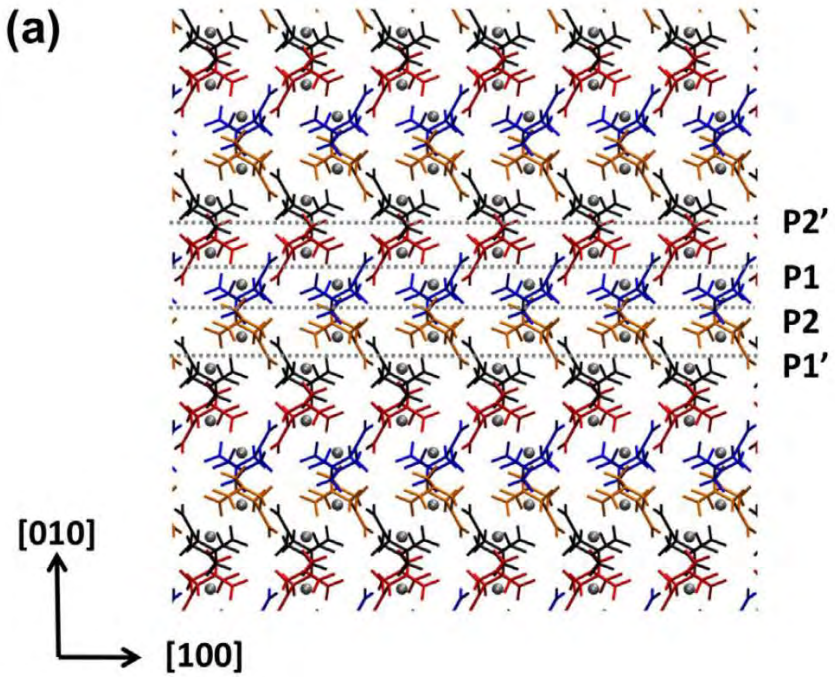

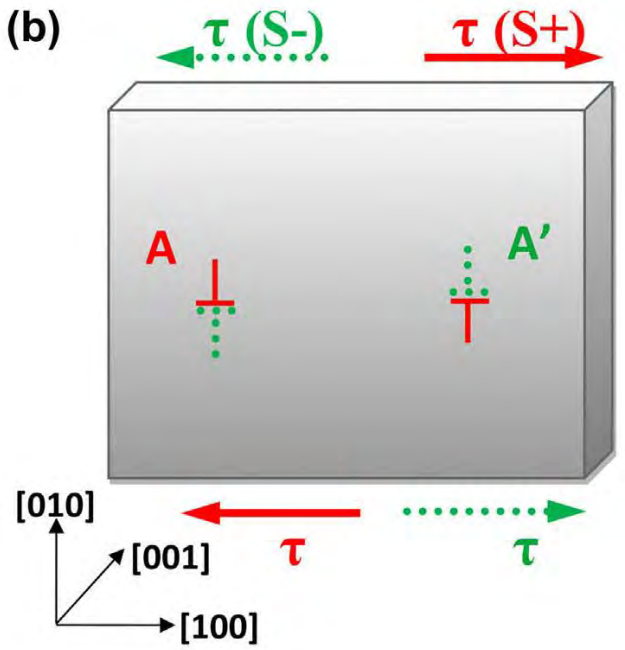

(d) Rotational defects in RDX
-Identification of stable rotated molecules-

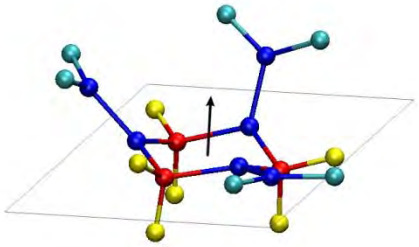

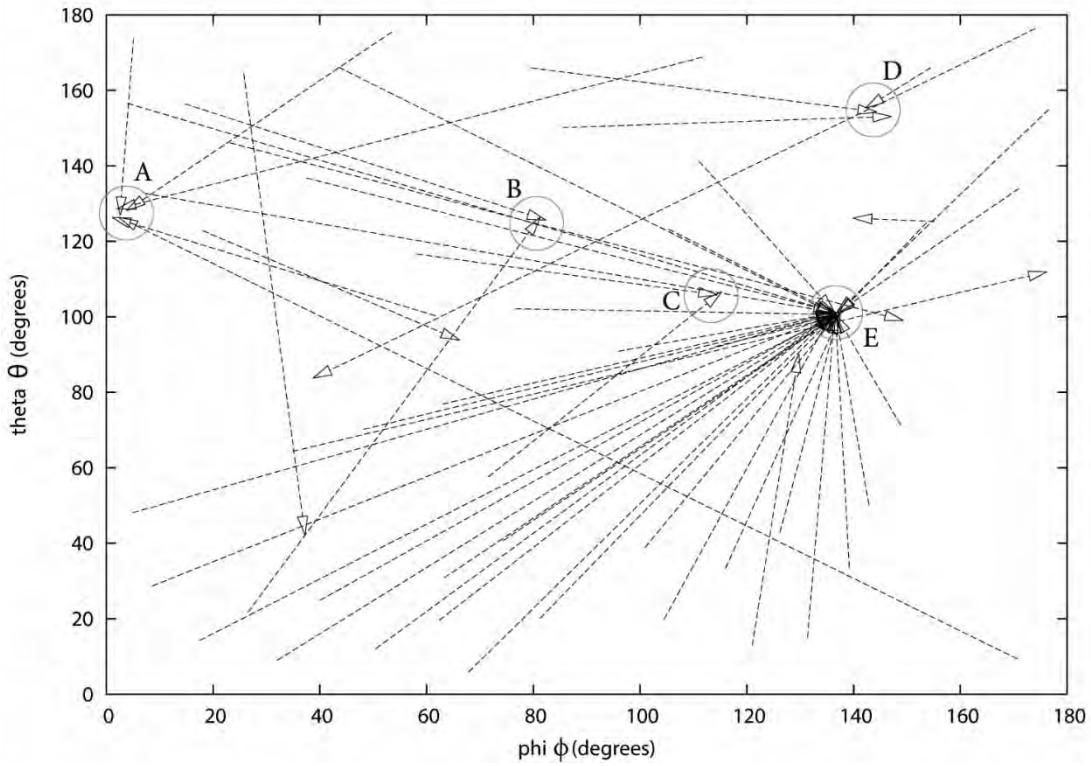

Map of the conformation (rotation) space. The arrows show how a molecule in a certain initial rotation state relaxes. The points to which multiple arrows point are attractors. All states labeled A to E are stable at low temperature, but convert to the perfect crystal orientation upon annealing at room temperature.

(d) Rotational defects in RDX
-Four stable rotational defects-

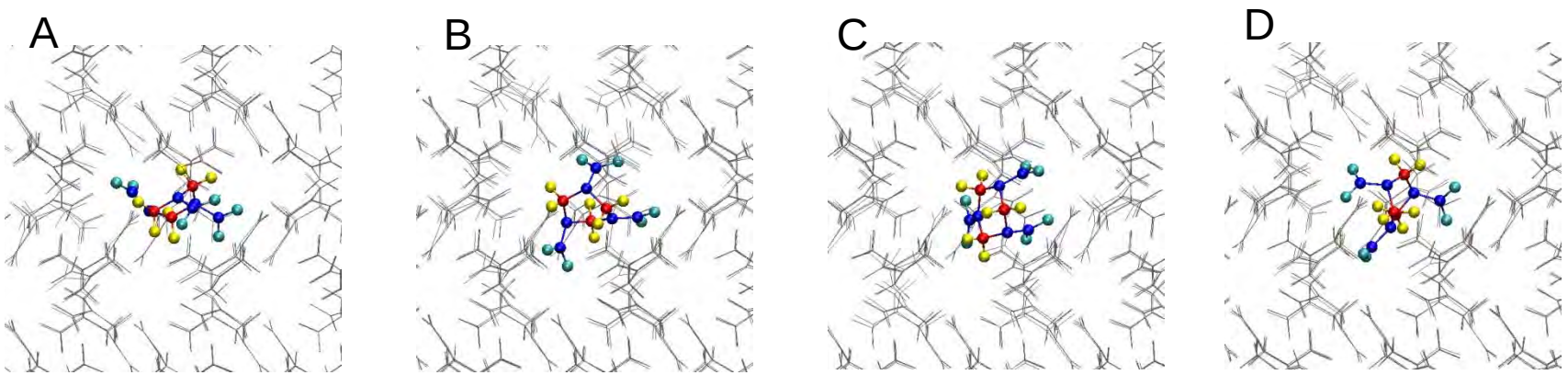

Four configurations of rotated molecules (rotational point defects) which are stable at low temperatures and which correspond to the 4 attractors of the map of slide 13. The fifth point on that map represents the perfect crystal orientation.

(d) Rotational defects in RDX
-Rotational defects are present at dislocation cores-

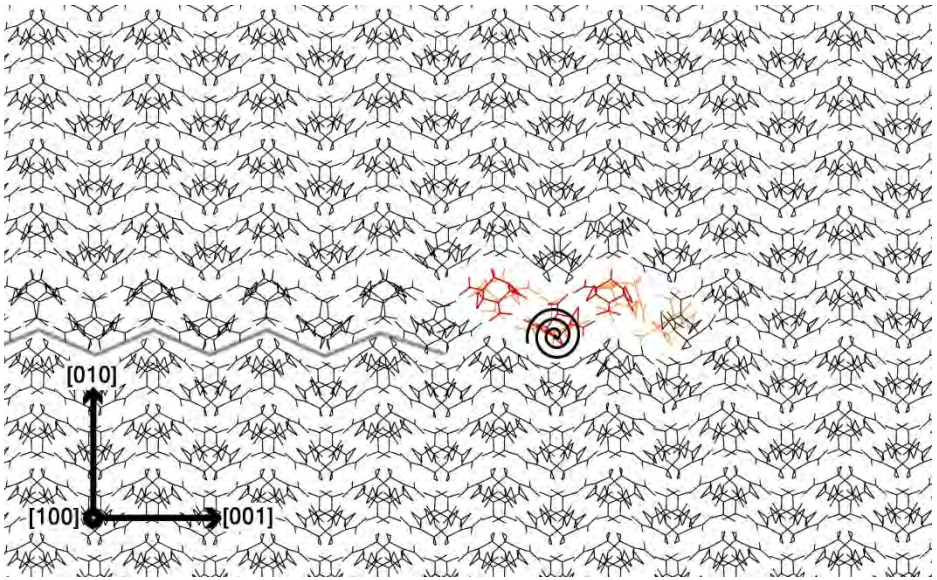

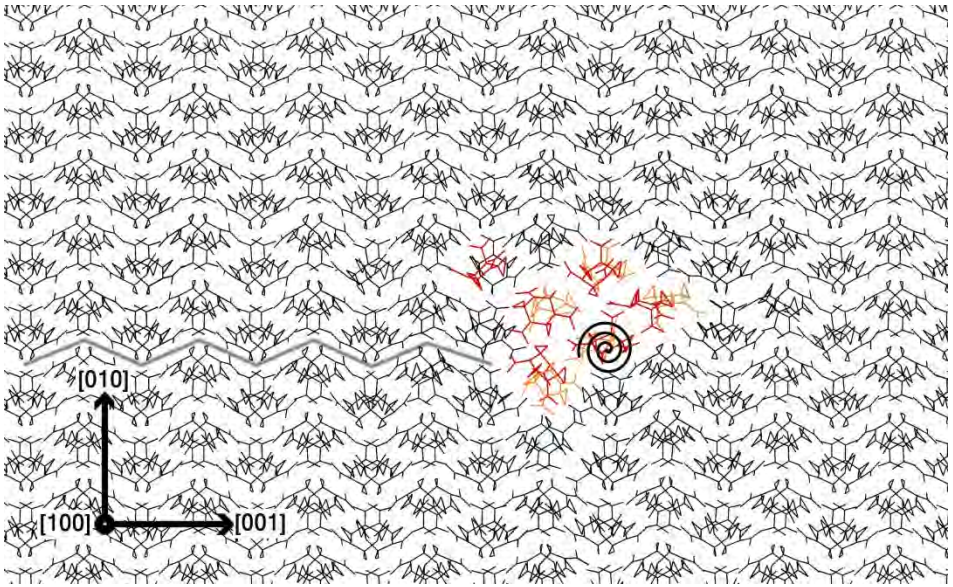

Edge and screw dislocation cores and rotational defects shown in color in the core region. These defects are stable in the cores even at room temperature. When the dislocation moves away, the defects heal back and disappear. This process takes a time comparable with the time required for the next dislocation moving in the same glide plane to arrive at the same location. Hence, we conjecture that these structures interact strongly with dislocations.

(d) Rotational defects in RDX
lectron charge density redistribution in rotational defects-

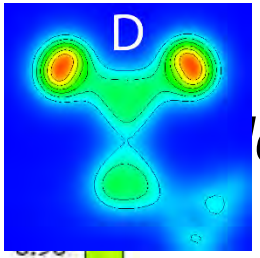

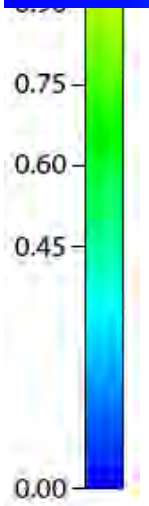

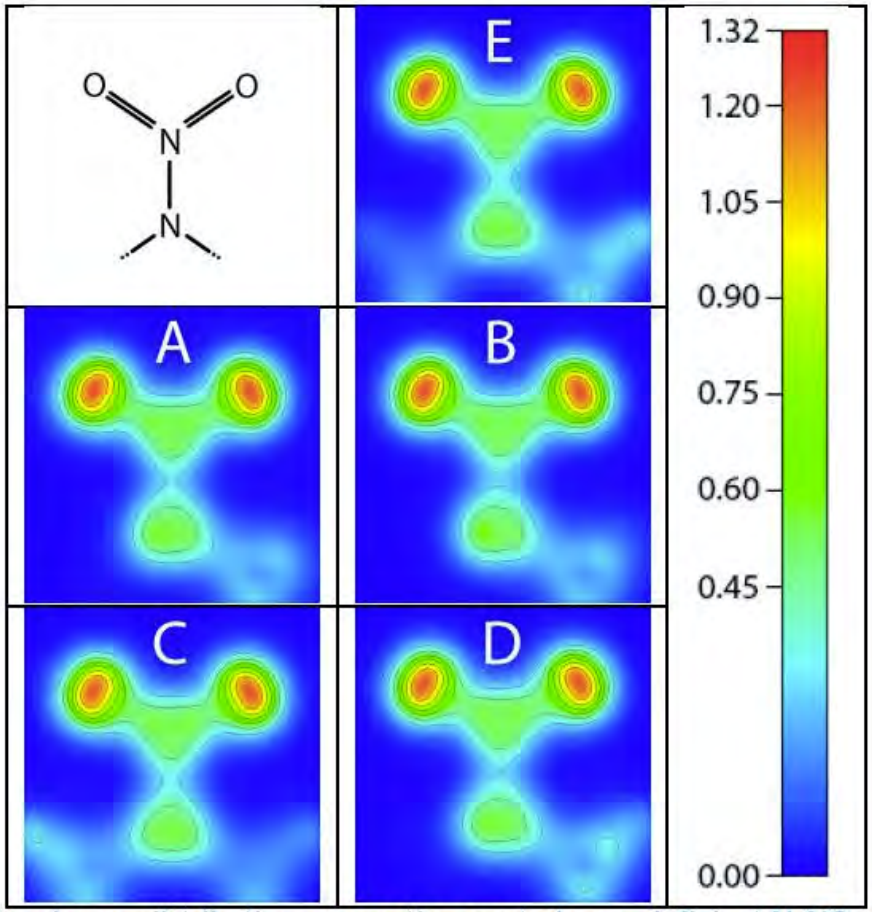

Electron charge distribution across the most charge deficient N-NO_2 groups in the perfect crystal (E) and Defect (A-D) molecules. The color scales from 0 to 1.32 (Bohr^3) with contours at 0.45 to 1.20 in multiples of 0.15. All defects display density reduction at the mid-point of the N-N bond, with Defect B having the largest deficiency.

(d) Rotational defects in RDX
-Identification of rotational defects using Raman-

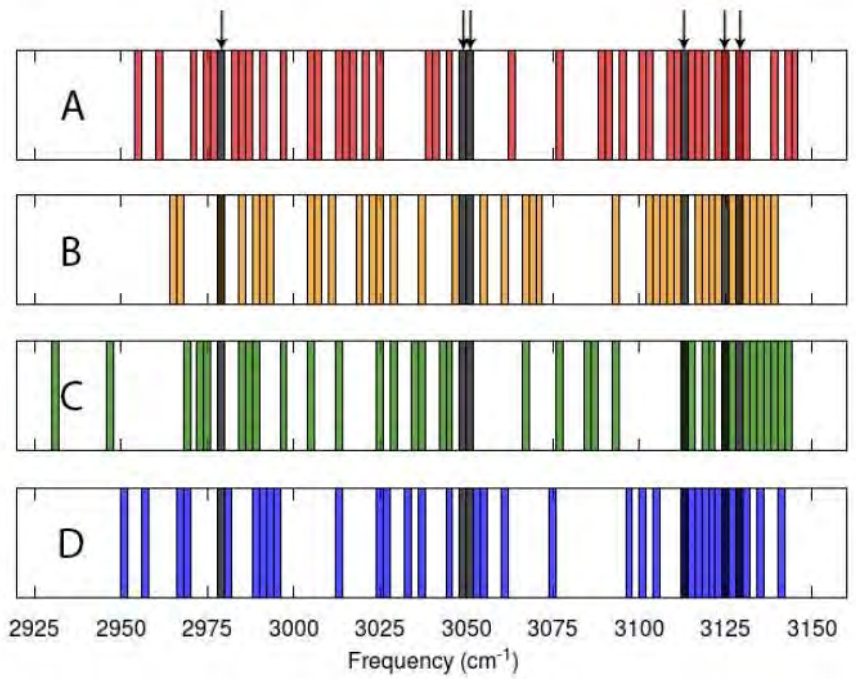

Splitting of high frequency Raman active modes in the presence of rotational defects of type A to D. The modes of defective crystals are shown in color, while those of the perfect crystal are shown in black (and arrows)

(e) Coarse grained models of RDX crystal -Hierarchy of models considered-

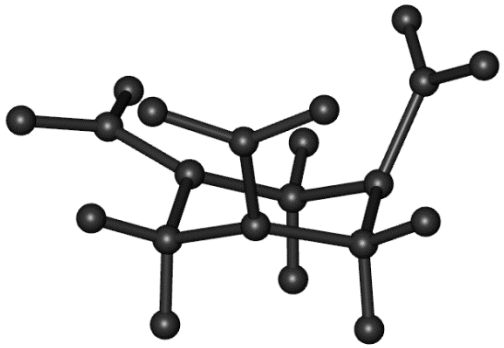

Model I: Fully flexible

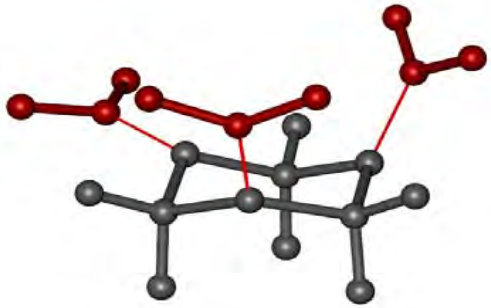

Model II: Ring flexible, N-N bonds rigid and nitro groups rigid

Increasing coarse graining level

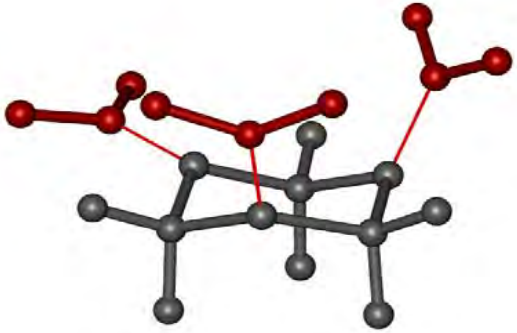

Model III: Ring flexible, but bonds very stiff axially. Nitro groups rigid but can move relative to the ring.

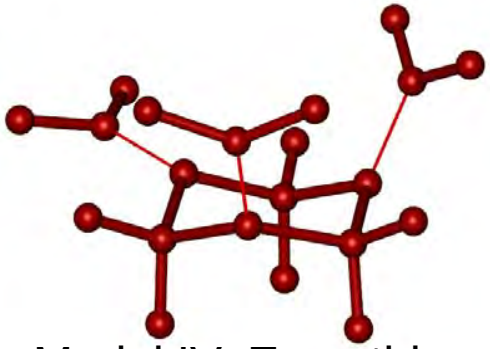

Model IV: Everything rigid except the nitro groups (which are rigid) can move relative to the ring

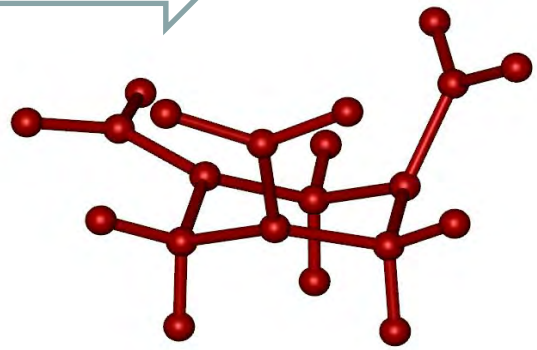

Model V: Fully rigid

Increasing coarse graining level

Hierarchy of coarse grained models developed in this work

(e) Coarse grained models of RDX crystal -Effect of coarse graining on elastic constants-

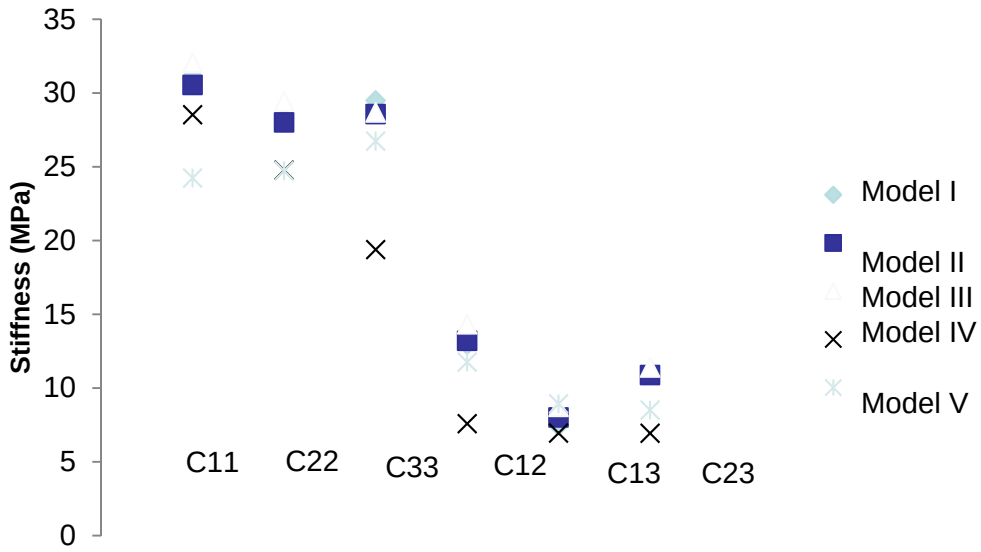

Prediction of crystal elasticity using the 6 models defined in slide 5.

(e) Coarse grained models of RDX crystal -Effect of coarse graining on lattice parameters and bulk modulus-

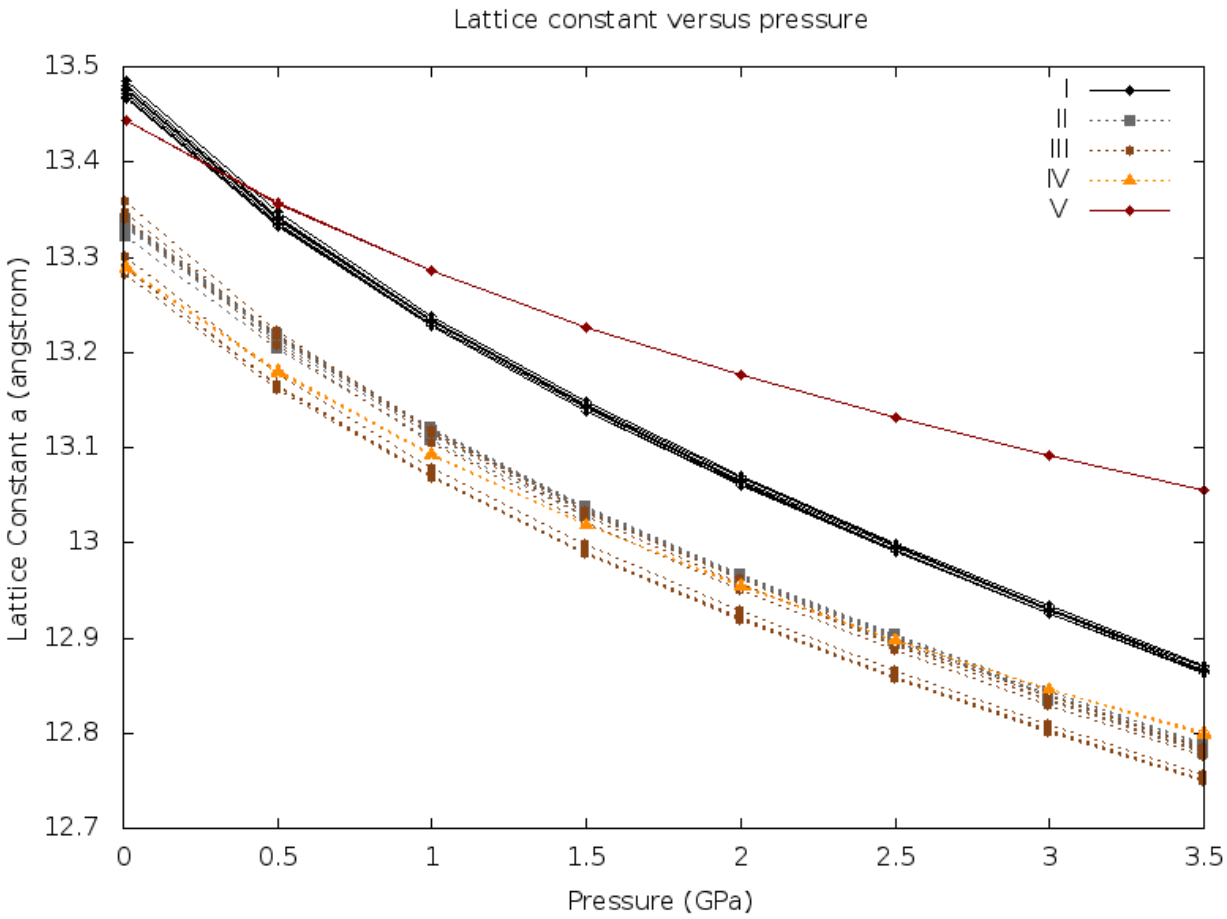

Variation of one of the lattice parameters (in Angstroms) with pressure, as predicted by the 5 coarse grained models.

(e) Coarse grained models of RDX crystal -Effect of coarse graining on thermal expansion-

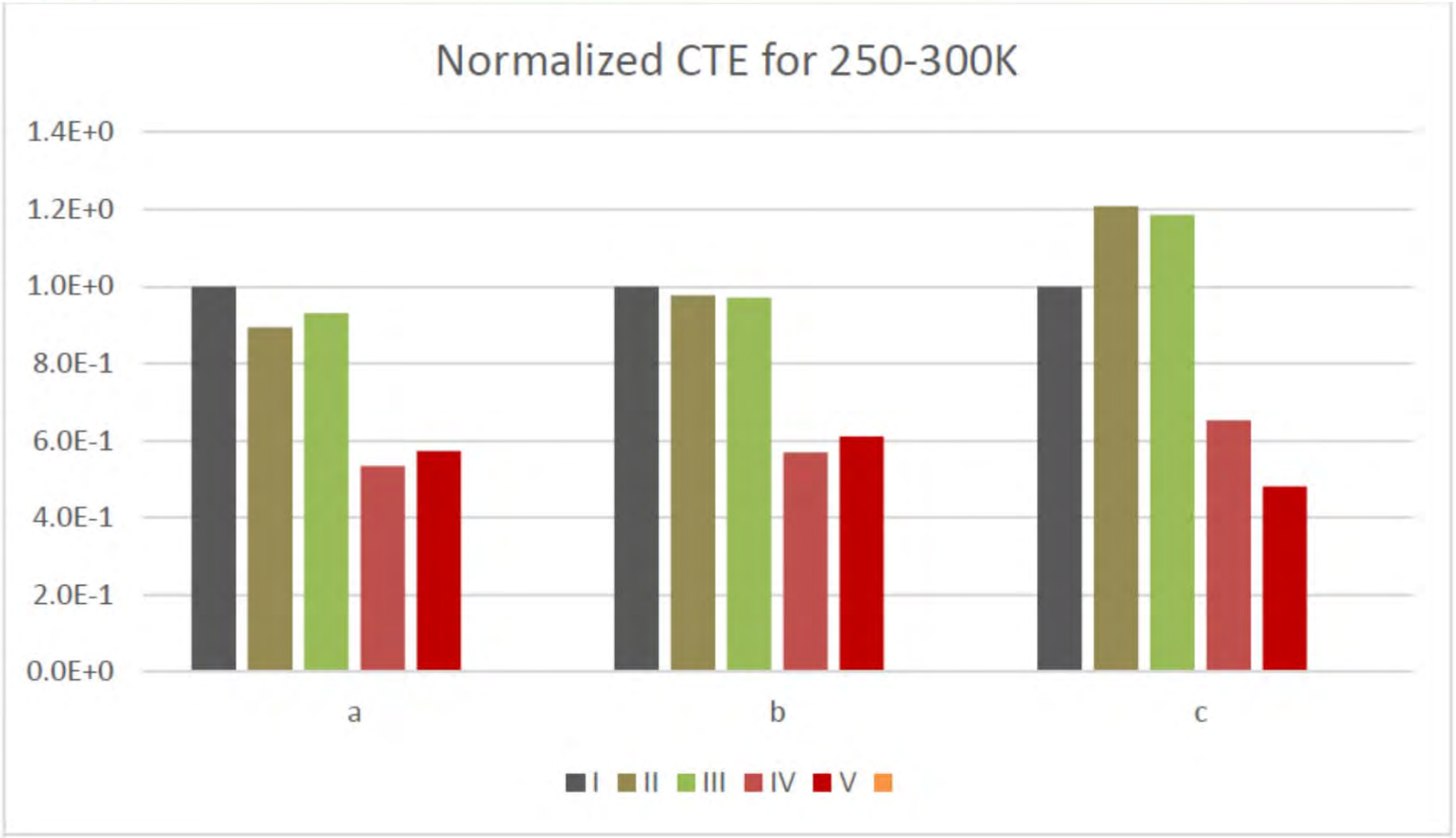

Variation of the CTE (normalized with reference model I) in three principal directions of the crystal at zero pressure and for all coarse grained models.